Available online at www.sciencedirect.com

SciVerse ScienceDirect

Ceramics International 39 (2013) 6215–6221

CERAMICS INTERNATIONAL

www.elsevier.com/locate/ceramint

Mechanical properties of graphene platelet-reinforced alumina ceramic composites

Jian Liu[a], Haixue Yan[b], Kyle Jiang[a,*]

[a]School of Mechanical Engineering, University of Birmingham, Birmingham B15 2TT, UK
[b]School of Engineering and Materials Science, Queen Mary, University of London, London E1 4NS, UK

Received 4 December 2012; received in revised form 13 January 2013; accepted 14 January 2013
Available online 21 January 2013

Abstract

Alumina (Al_2O_3) ceramic composites reinforced with graphene platelets (GPLs) were prepared using Spark Plasma Sintering. The effects of GPLs on the microstructure and mechanical properties of the Al_2O_3 based ceramic composites were investigated. The results show that GPLs are well dispersed in the ceramic matrix. However, overlapping of GPLs and porosity within ceramics are observed. The flexural strength and fracture toughness of the GPL-reinforced Al_2O_3 ceramic composites are significantly higher than that of monolithic Al_2O_3 samples. A 30.75% increase in flexural strength and a 27.20% increase in fracture toughness for the Al_2O_3ceramic composites have been achieved by adding GPLs. The toughening mechanisms, such as pull-out and crack deflection induced by GPLs are observed and discussed.

Keywords: A. Sintering; B. Composites; C. Mechanical properties; C. Toughness and toughening

1. Introduction

In the last decade, carbon fillers, such as carbon fibres and carbon nanotubes (CNTs) have been widely investigated to improve the mechanical and electrical properties of a variety of host materials [1–15]. Especially CNTs with high tensile strength and stiffness, good flexibility, and low density make themselves attractive for many applications and technologies. Various researches have been carried out to incorporate CNTs into ceramic matrices to produce tough as well as highly stiff ceramic composites. A number of studies have been reported. Yamamoto et al. [14]used a precursor method to fabricate the CNT/Al_2O_3 composites and achieved a 25% increase in fracture toughness, compared to pure Al_2O_3. Bocanegra–Bernal et al. [2] studied the effects of carbon nanotubes on the properties of ZrO_2 toughened Al_2O_3 (ZTA) composites and reported a 44% increase in fracture toughness over the pure ZTA.

Graphene, the two dimensional counterpart of CNTs consisting of a one-atom thick layer of carbon atoms arranged in a honeycomb lattice, has imposed itself with many outstanding properties and can be a promising alternative of carbon nanotubes in various applications [16–26]. In contrast to monolayer graphene, GPLs are formed by several layers of graphene with thickness of up to100 nm[27], and are referred in literature as graphene nanosheets (GNS), multilayer graphene nanosheets (MGN) or graphene nanoplatelets (GNPs). GPLs have a large specific surface area, two dimensional high aspect ratio geometry, and outstanding mechanical properties, which make them excellent potential nanofillers in composite materials. Studies have shown that the mechanical properties of ceramic based composites can be significantly improved with relatively low nanofiller loading. Wang et al. [28] used spark plasma sintering(SPS) to prepare graphene nanosheet/ Al_2O_3 composite and a 53% increase in fracture toughness was obtained with addition of 2 wt% of GPLs. Walker et al. [29] employed aqueous colloidal processing methods to obtain uniform and homogeneous dispersions of GPLs and Si_3N_4 ceramic particles which were densified using SPS. The measured fracture toughness of 6.6 MPa $m^{1/2}$ for the composite with 1.5 vol%

*Corresponding author. Tel.: +44 0 121 414 6800; fax: +44 0 121 414 7484.
E-mail address: k.jiang@bham.ac.uk (K. Jiang).

0272-8842/$ - see front matter © 2013 Elsevier Ltd and Techna Group S.r.l. All rights reserved.
http://dx.doi.org/10.1016/j.ceramint.2013.01.041

of GPLs was 136% higher than that of monolithic Si_3N_4. Ján Dusza et al. [30] prepared GPL-reinforced Si_3N_4 composites containing 1 wt% GPLs using hot isostatic pressing and reported an increase of about 44% in fracture toughness over the pure Si_3N_4. Jian Liu et al. [31]employed the SPS to fabricate GPL/ZTA composites with addition of 0.81 vol% GPLs and find an increase of nearly 40% in fracture toughness.

Structural ceramics, such as alumina, are widely used in the materials industry and have potential applications covering high speed cutting tools, dental implants, chemical and electrical insulators, wear resistance parts and various coatings. These applications arise from their high hardness, chemical inertness and high electrical and thermal insulation properties [1,32–38]. However, their applications are significantly restricted by brittleness and fabrication difficulties. The most crucial property is fracture toughness, which indicates the resistance to crack initiation and propagation. Improving fracture toughness is therefore very important to enable broader applications of such ceramics.

In this study, we are aiming to produce alumina composites reinforced with GPLs and the mechanical properties of the new structural materials are analysed. SPS processes are used to condense ceramic samples and protect the graphene fillers from oxidation. The microstructures of the achieved GPL-reinforced ceramic composites are presented and their mechanical properties are characterised. The effect of percentage of GPLs on the mechanical properties of the ceramic composites is discussed.

2. Experimental procedure

2.1. Starting materials

α-alumina powder (Inframat Advanced Materials, Farmington, CT, USA) with a purity of 99.85%, an average particle size of 150 nm and a surface area of 10 m^2/g was used in this study. GPLs were procured from Graphene Industries Ltd. A general approach to produce the GPL is via rapid thermal expansion/exfoliation of graphite that has been intercalated using sulphuric acid [39]. The resultant platelets are stacks of graphene sheets about 6–8 nm in thickness and 15–25 μm in level dimensions. An SEM image of the obtained GPL is shown in Fig. 1.

2.2. Powder mixture preparation

Appropriate quantities of GPLs were first dispersed in DMF and sonicated for one hour.

Al_2O_3 (50 g) powder was added and then the mixture was further sonicated for 10 min. This was followed by a ball milling procedure at 100 rpm in a planetary ball mill (PM 100, Retsch, UK) for 4 h. The milling was carried out in a cylindrical zirconia container using ZrO_2 balls under a ball-to-powder weight ratio of 2. The milled slurry mixture was dried at 90 °C in an oven for 3 days. The dried powder mixture was ground and sieved using a 140 mesh.

2.3. Spark plasma sintering and characterisation

Bulk composite samples were sintered using a SPS process (HPD 25/1 furnace, FCT Systeme, Germany). The powder mixtures were poured into a graphite die of 40 mm in diameter. A sheet of graphitic paper was placed between the punch and the powder and between the die and the powder for easy removal of the sintered sample. The sintering process was conducted under a vacuum of 5 Pa. A uniaxial pressure of 50 MPa was applied throughout the sintering cycle. The process was started by raising the temperature to 400 °C using a preset heating programme. The sintering temperature was increased to the range of 1500–1550 °C at a rate of 100 °C/min. A 3 min soaking time was used during the sintering. The temperature was measured and controlled using an optical pyrometer. Shrinkage, displacement, heating current, and voltage were also recorded during the sintering processes. Afterwards, the samples were ground and polished to 0.5 μm using SiC paper and diamond suspension. The bulk density of the samples was measured by the Archimedes method with ethanol as the immersion medium using densities of 3.97 and 2.1 g m^{-3} for Al_2O_3 and GPL. The relative density was calculated by dividing the bulk density with the theoretical density of the powder mixture. Vicker

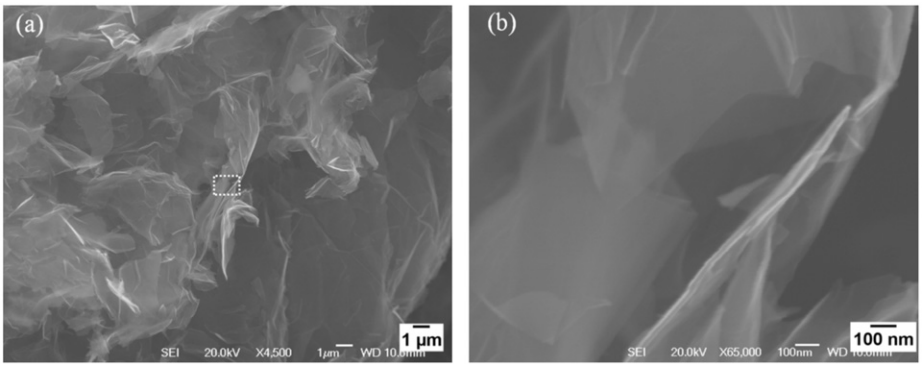

Fig. 1. (a) A SEM image of GPLs and (b) the GPLs with higher magnification.

hardness tests were carried out using a 2 kg force. Fracture surfaces of the coated samples were determined by scanning electron microscopy (SEM). Instron mechanical tester in Science City Advanced Materials II Laboratory at Birmingham was used to determine the flexural strength and fracture toughness of the ceramic composites. The fracture toughness was measured by the single edge v-notched beam (SEVNB) method under ambient conditions. The size of test specimens was 3 mm (width) × 4 mm (thickness) × 36 mm (length). A notch in the centre part of the test specimen was cut by a diamond wheel and further sharpened using a razor blade with the aid of diamond paste up to 1 μm. The tip radii of the notches were $< \sim 10$ μm, as shown in Fig. 2. The final depths of the notches range from 1 to1.2 mm.A span length of 30 mm and crosshead speed of 0.05 mm/min were applied in the toughness tests. Five samples were tested for each material. Flexure strength was measured using three point bending, in which the size of test specimens was 1.5 mm (width) × 2 mm(thickness) × 25 mm (length). The span length and crosshead speed for the strength tests were 20 mm and 0.05 mm min^{-1}. Five bars were tested for each material.

3. Results and discussion

3.1. Microstructure of the 'as-prepared' samples

Sintered ceramic samples were fractured and their microstructures were examined. Fig. 3 shows the SEM images of fracture surfaces of the samples with and without GPLs. It can be seen that the GPLs are well dispersed in the ceramic matrix. From the fracture surfaces, which present a mainly

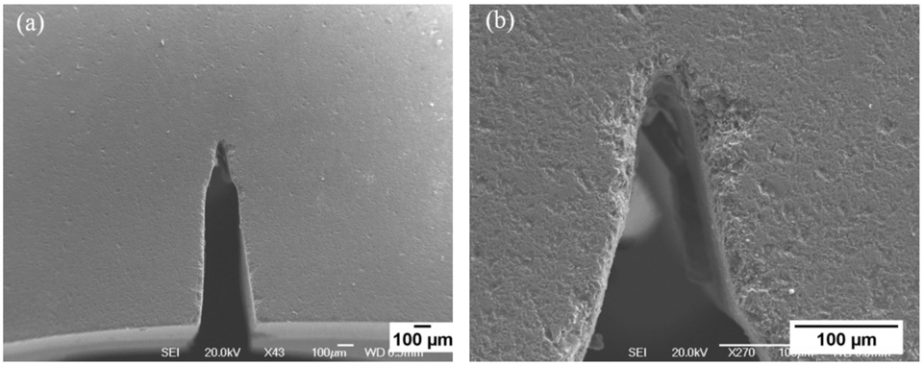

Fig. 2. (a) A SEM image of specimen with sharpened notch and (b) the magnified part of the notch tip.

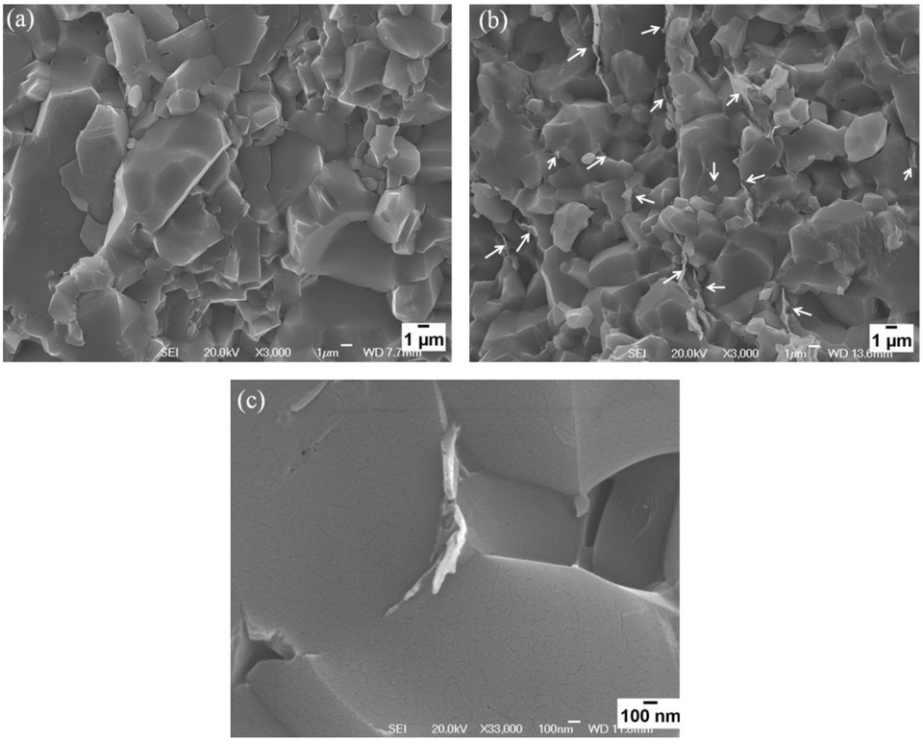

Fig. 3. SEM images of fracture surfaces of the sintered samples. (a) is the sample without GPLs. (b) and (c) are the samples with GPLs. The arrows indicate GPLs embedded in the matrix.

intergranular fracture mode, debonded GPLs pulled out from the ceramic matrix can be observed. In addition, in comparison to the pure Al_2O_3 sample where large and uneven grains are observed, GPL composites exhibit more uniform microstructures. Meanwhile, as shown in Fig. 3b and c, GPLs tend to be distributed between ceramic grain boundaries and prevent migration of grain boundaries, resulting in a refinement of microstructure.

3.2. Mechanical properties of sintered samples

Mechanical properties of the GPL-reinforced Al_2O_3 composites and the monolith Al_2O_3 are compiled into Table 1. It can be seen that all the samples are fully densified during the SPS process and the hardness does not vary very much with the addition of GPLs. Furthermore, mechanical properties of all the composites have been significantly improved. Especially flexural strength and fracture toughness of 0.38 vol% GPLs-Al_2O_3 composites have increased by 30.75% and 27.20% over the monolithic Al_2O_3, reaching their maximum values of 523 ± 30 MPa and 4.49 ± 0.33 MPa $m^{1/2}$ respectively. Such increases are comparable to CNT-reinforced ceramics [9,13,14,40]. However, further increase of GPLs in the ceramics causes degradation of mechanical properties.

3.3. Effect of GPLs in the GPL/ Al_2O_3 composites

Similar to conventional fibre-reinforced ceramics, toughening mechanisms, such as pull-out and crack deflection, are observed on fracture surfaces of the ceramic composites reinforced with GPLs. Fig. 4 shows a large GPL runs along the grain boundary and forms a large area of interface (Fig. 4a) and small graphene sheets are securely anchored within the grain boundaries of the matrix microstructure (Figs. 4b and c).

It is expected that when the consolidation proceeds during the sintering, graphene sheets conform with the force applied by their neighbouring matrix grains and are bent and embedded between the grains. Such close contact between the matrix grains and graphene enables the platelets to anchor at and bind with matrix grains, which results in increased contact area. Fracture toughness of the ceramics is therefore believed to be greatly improved due to the interfacial friction in the interface between the graphene sheet and ceramic matrix and the energy to pull out a graphene sheet is expected to be much greater than to pull out a nano fibre or carbon nanotube.

In addition, it is found that GPLs deflect cracks, just as fibres do in ceramics. As shown in Fig. 4e and f, when a crack propagates and meets with a graphene platelet, it is arrested and deflected in-plane. It is believed that such a crack deflection mechanism would create a more tortuous path to release stress, which helps increase the fracture toughness.

Usually the reinforcing efficiency of the nanoscale fillers in ceramic is mainly determined by the following factors: (1) the intrinsic mechanical properties of the filler material, (2) the efficiency of load transfer at the interface of matrix and filler, and (3) the dispersion level of the nanoscale filers in the ceramic matrix. In the GPL-reinforced Al_2O_3 composites, GPLs with high Young's modulus and large specific area are well dispersed in the ceramic matrix. They are either distributed in the grain boundary (Fig. 4a, b and c) helping transfer the load from the ceramic matrix or embedded within the grains (Fig. 4d) reinforcing the ceramic matrix, which significantly improves the flexural strength of the composites.

3.4. Porosity induced by GPLs in the GPL/ Al_2O_3 composites

Although nearly fully densified samples are obtained, some elongated pores are observed, as shown in Fig. 5. Similar results have been reported in CNT-reinforcing metal oxide composites and GPL-silicon nitride ceramics [7,41,42]. Similar to CNTs, GPLs tend to be distributed in the grain boundaries of the ceramic matrix, which hampers the densification process. Pores are likely to be formed when a good bonding between GPLs and ceramic matrix are not formed, which make it difficult to accommodate different shrinkages in the interface between GPLs and ceramic matrix during a cooling process. In addition, these pores are believed to be the origins of the fractures and weaken the strength of ceramic composites, which explains the fact that excessive addition of GPLs leads to less strong composites. An optimum percentage of GPLs in a GPL–reinforced ceramics can result in the maximum flexural strength.

Although GPLs shown in Fig. 3 are well dispersed in the ceramic matrix, overlapping of GPLs is observed in Fig. 5. The single platelets used in the research are 8–10 nm thick, whereas the overlapped platelets are 20–110 nm thick, which indicates moderate agglomeration of GPLs occurs

Table 1
Mechanical properties of the GPL-reinforced Al_2O_3 composites and the monolith Al_2O_3.

Samples	Temperature (°C)	Relative density (%)	Hardness (GPa)	Flexural strength (MPa)	Fracture toughness (MPa $m^{1/2}$)
Pure Al_2O_3	1500	100	18.04 ± 0.76	400 ± 25	3.53 ± 0.25
Al_2O_3/0.38 vol% GPLs	1500	99.58	17.66 ± 0.84	523 ± 30	4.49 ± 0.33
Al_2O_3/0.76 vol% GPLs	1550	99.92	17.46 ± 0.49	485 ± 23	4.11 ± 0.44
Al_2O_3/1.33% vol GPLs	1550	99.87	16.32 ± 0.44	464 ± 26	3.94 ± 0.36

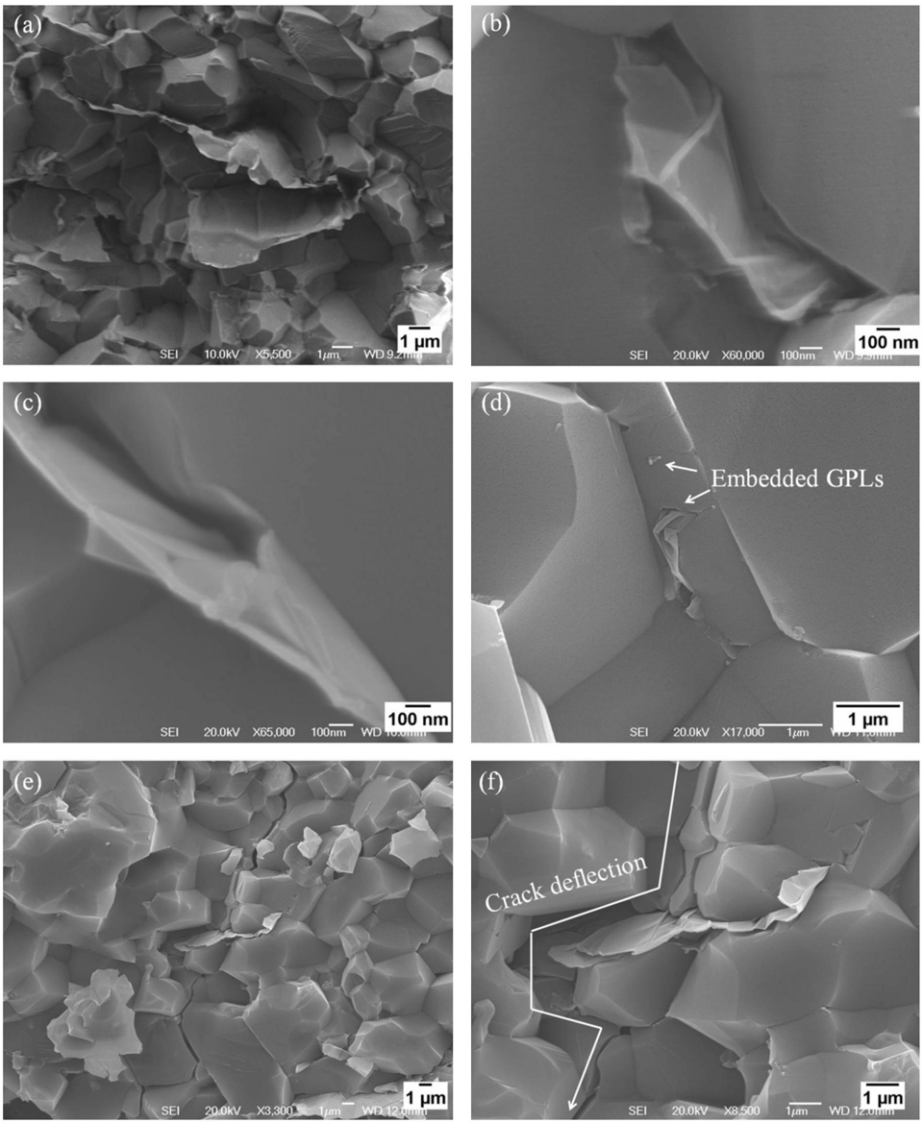

Fig. 4. SEM images of fracture surface of GPL-reinforced Al_2O_3 composite showing the toughening and reinforcing mechanisms.

in the fabrication process. The presence of aggregation is believed to drastically affect the mechanical properties of composite materials for the reason that in comparison with thin GPLs, more pores would be formed in the interface between thick GPLs and ceramic matrix because of the degraded flexibility of the thick GPLs. These pores undermine the role of crack deflection toughening mechanism for they result in a decreased contact area between the ceramic matrix and GPLs, as well as initiate cracks, along which stress is released in a less efficient way. Meanwhile, when GPLs act as a pull-out role, the pores weaken the interfacial friction in the interface between the ceramic matrix and GPLs. Therefore aggregates would degrade strengthening as well as toughening effects of the GPLs and cause detrimental effect to mechanical properties of the composites.

Obviously dispersion level of nanostructures in a matrix is one of the key factors in defining the mechanical properties of the composites. It is necessary to achieve dispersion of the GPLs as complete as possible to obtain ceramic composites with excellent mechanical properties.

4. Conclusions

This paper reports a study of the preparation and characterisation of GPL/ Al_2O_3 ceramic composites. GPLs were first dispersed in DMF and then mixed with Al_2O_3 in a ball milling process. Nearly fully densified samples are obtained after spark plasma sintering. Analysis of the results shows that GPLs are well dispersed in the ceramic matrix microstructure. Local overlap of GPLs and porosity within the ceramics are observed. The flexural strength and fracture toughness of the GPL-reinforced Al_2O_3 ceramic composites are significantly higher than that of monolithic Al_2O_3 sample. The addition of only 0.78 vol% GPLs to alumina results in 30.75% and 27.20% simultaneously increases in flexural strength (523 ± 30 MPa) and fracture toughness (4.49 ± 0.33 MPa $m^{1/2}$), respectively,

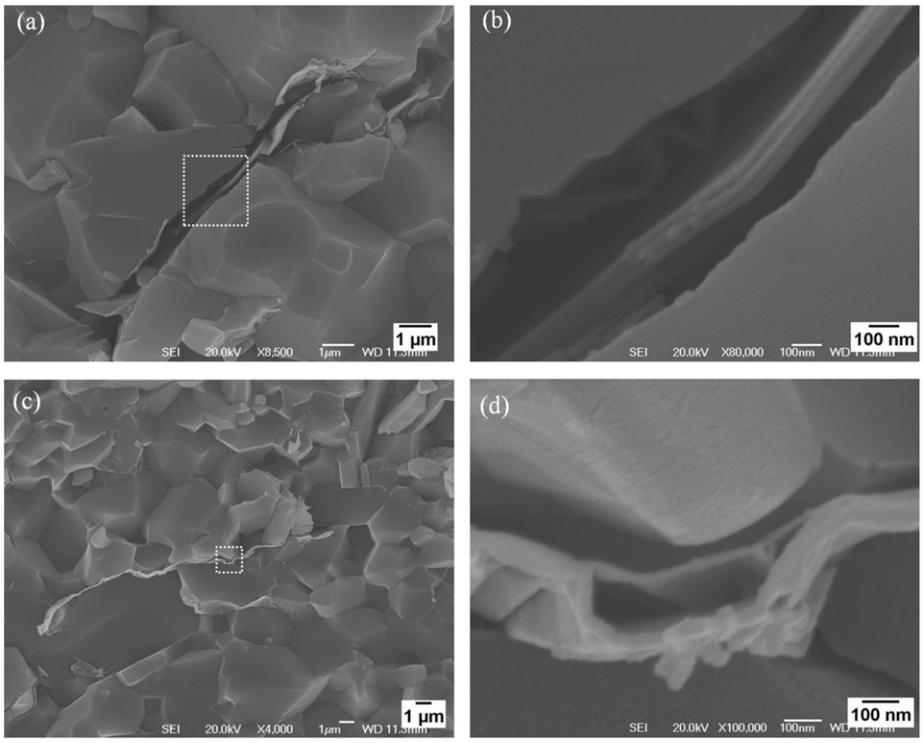

Fig. 5. SEM images of fracture surface of GPL-reinforced Al_2O_3 composite showing the pores and agglomeration of GPLs. (b) and (d) are the magnified part of white square areas in (a) and (c).

indicating enhanced stress transfer capability from the alumina to the GPLs. With increasing GPLs fraction, the porosity increased, and adversely affected the flexure strength and fracture toughness because of pores working as fracture initiation sites. Toughening mechanisms responsible for the increase in fracture toughness are pull-out and crack deflection. The presented work shows graphene nanofillers have potential to improve the fracture toughness of ceramic composites considerably and lead to a variety of light and strong ceramics to suit engineering applications.

Acknowledgement

This work was supported, in part, by NSFC State Key Project 90923001 and Project B12016 of Programme 111. Authors would like to thank Dr James Bowen for the help with the Instron mechanical tester.

References

[1] I. Ahmad, H.Z. Cao, H.H. Chen, H. Zhao, A. Kennedy, Y.Q. Zhu, Carbon nanotube toughened aluminium oxide nanocomposite, Journal of the European Ceramic Society 30 (4) (2010) 865–873.

[2] M.H. Bocanegra-Bernal, J. Echeberria, J. Ollo, A. Garcia-Reyes, C. Dominguez-Rios, A. Reyes-Rojas, A. Aguilar-Elguezabal, A comparison of the effects of multi-wall and single-wall carbon nanotube additions on the properties of zirconia toughened alumina composites, Carbon 49 (5) (2011) 1599–1607.

[3] A.R. Boccaccini, B.J.C. Thomas, G. Brusatin, P. Colombo, Mechanical and electrical properties of hot-pressed borosilicate glass matrix composites containing multi-wall carbon nanotubes, Journal of Materials Science 42 (6) (2007) 2030–2036.

[4] S.I. Cha, K.T. Kim, K.H. Lee, C.B. Mo, S.H. Hong, Strengthening and toughening of carbon nanotube reinforced alumina nanocomposite fabricated by molecular level mixing process, Scripta Materialia 53 (7) (2005) 793–797.

[5] Y.L. Chen, B. Liu, Y. Huang, K.C. Hwang, Fracture Toughness of Carbon Nanotube-Reinforced Metal- and Ceramic-Matrix Composites, Journal of Nanomaterials (2011).

[6] M. Estili, H. Kwon, A. Kawasaki, S. Cho, K. Takagi, K. Kikuchi, M. Kawai, Multiwalled carbon nanotube-reinforced ceramic matrix composites as a promising structural material, Journal of Nuclear Materials 398 (1-3) (2010) 244–245.

[7] J.P. Fan, D.M. Zhuang, D.Q. Zhao, G. Zhang, M.S. Wu, F. Wei, Z.J. Fan, Toughening and reinforcing alumina matrix composite with single-wall carbon nanotubes, Applied Physics Letters 89 (12) (2006).

[8] Y.C. Fan, L.J. Wang, J.L. Li, J.Q. Li, S.K. Sun, F. Chen, L.D. Chen, W. Jiang, Preparation and electrical properties of graphene nanosheet/Al2O3 composites, Carbon 48 (6) (2010) 1743–1749.

[9] C.N. He, F. Tian, S.J. Liu, A carbon nanotube/alumina network structure for fabricating alumina matrix composites, Journal of Alloys and Compounds 478 (1–2) (2009) 816–819.

[10] F. Inam, H. Yan, M.J. Reece, T. Peijs, Dimethylformamide: an effective dispersant for making ceramic-carbon nanotube composites, Nanotechnology 19 (19) (2008).

[11] F. Inam, H. Yan, M.J. Reece, T. Peijs, Structural and chemical stability of multiwall carbon nanotubes in sintered ceramic nanocomposite, Advances in Applied Ceramics 109 (4) (2010) 240–245.

[12] H. Kwon, S.C. Cho, M. Leparoux, A. Kawasaki, Dual-nanoparticulate-reinforced aluminum matrix composite materials, Nanotechnology 23 (22) (2012).

[13] T. Wei, Z.J. Fan, G.H. Luo, F. Wei, A new structure for multi-walled carbon nanotubes reinforced alumina nanocomposite with high strength and toughness, Materials Letters 62 (4-5) (2008) 641–644.

[14] G. Yamamoto, M. Omori, T. Hashida, H. Kimura, A novel structure for carbon nanotube reinforced alumina composites with improved mechanical properties, Nanotechnology 19 (31) (2008).
[15] L.P. Zhao, Y.J. Li, X.J. Cao, J.C. You, W.Y. Dong, Multifunctional role of an ionic liquid in melt-blended poly(methyl methacrylate)/multi-walled carbon nanotube nanocomposites, Nanotechnology 23 (25) (2012).
[16] The rise and rise of graphene, Nature Nanotechnology, 5 (11), 2010, 755–755.
[17] Z.G. Cheng, Q.Y. Zhou, C.X. Wang, Q.A. Li, C. Wang, Y. Fang, Toward intrinsic graphene surfaces: a systematic study on thermal annealing and wet-chemical treatment of sio2-supported graphene devices, Nano Letters 11 (2) (2011) 767–771.
[18] A.K. Geim, K.S. Novoselov, The rise of graphene, Nature Materials 6 (3) (2007) 183–191.
[19] S. Iijima, Helical microtubules of graphitic carbon, Nature 354 (6348) (1991) 56–58.
[20] L. Liao, Y.C. Lin, M.Q. Bao, R. Cheng, J.W. Bai, Y.A. Liu, Y.Q. Qu, K.L. Wang, Y. Huang, X.F. Duan, High-speed graphene transistors with a self-aligned nanowire gate, Nature 467 (7313) (2010) 305–308.
[21] S. Park, J.H. An, I.W. Jung, R.D. Piner, S.J. An, X.S. Li, A. Velamakanni, R.S. Ruoff, Colloidal suspensions of highly reduced graphene oxide in a wide variety of organic solvents, Nano Letters 9 (4) (2009) 1593–1597.
[22] P. Pasanen, M. Voutilainen, M. Helle, X.F. Song, P.J. Hakonen, Graphene for future electronics, Physica Scripta T146 (2012).
[23] H. Seema, K.C. Kemp, V. Chandra, K.S. Kim, Graphene–SnO_2 composites for highly efficient photocatalytic degradation of methylene blue under sunlight, Nanotechnology 23 (35) (2012).
[24] O. Tapaszto, L. Tapaszto, M. Marko, F. Kern, R. Gadow, C. Balazsi, Dispersion patterns of graphene and carbon nanotubes in ceramic matrix composites, Chemical Physics Letters 511 (4–6) (2011) 340–343.
[25] T. Yoon, W.C. Shin, T.Y. Kim, J.H. Mun, T.S. Kim, B.J. Cho, Direct measurement of adhesion energy of monolayer graphene as-grown on copper and its application to renewable transfer process, Nano Letters 12 (3) (2012) 1448–1452.
[26] S.E. Zhu, R. Shabani, J. Rho, Y. Kim, B.H. Hong, J.H. Ahn, H.J. Cho, Graphene-based bimorph microactuators, Nano Letters 11 (3) (2011) 977–981.
[27] J.M.Ján Dusza, Annamária Duszová, Lenka Kvetková, Martin Nosko, Péter Kun, Csaba Balázsi, Microstructure and fracture toughness of Si_3N_4+graphene platelet composites, Journal of the European Ceramic Society 32 (12) (2012) 3389–3397.
[28] K. Wang, Y.F. Wang, Z.J. Fan, J. Yan, T. Wei, Preparation of graphene nanosheet/alumina composites by spark plasma sintering, Materials Research Bulletin 46 (2) (2011) 315–318.
[29] L.S. Walker, V.R. Marotto, M.A. Rafiee, N. Koratkar, E.L. Corral, Toughening in graphene ceramic composites, ACS Nano 5 (4) (2011) 3182–3190.
[30] L. Kvetkova, A. Duszova, P. Hvizdos, J. Dusza, P. Kun, C. Balazsi, Fracture toughness and toughening mechanisms in graphene platelet reinforced Si_3N_4 composites, Scripta Materialia 66 (10) (2012) 793–796.
[31] J. Liu, H. Yan, M.J. Reece, K. Jiang, Toughening of zirconia/alumina composites by the addition of graphene platelets, Journal of the European Ceramic Society 32 (16) (2012) 4185–4193.
[32] D. Chakravarty, S. Bysakh, K. Muraleedharan, T.N. Rao, R. Sundaresan, Spark plasma sintering of magnesia-doped alumina with high hardness and fracture toughness, Journal of the American Ceramic Society 91 (1) (2008) 203–208.
[33] R.H.L. Garcia, V. Ussui, N.B. de Lima, E.N.S. Muccillo, D.R.R. Lazar, Physical properties of alumina/yttria-stabilized zirconia composites with improved microstructure, Journal of Alloys and Compounds 486 (1-2) (2009) 747–753.
[34] M. Ipek, S. Zeytin, C. Bindal, An evaluation of Al2O3-ZrO2 composites produced by coprecipitation method, Journal of Alloys and Compounds 509 (2) (2011) 486–489.
[35] J. Kishan, V. Mangam, B.S.B. Reddy, S. Das, K. Das, Aqueous combustion synthesis and characterisation of zirconia–alumina nanocomposites, Journal of Alloys and Compounds 490 (1-2) (2010) 631–636.
[36] B. Li, J.X. Deng, Addition of Zr–O–B compounds to improve the performances of alumina matrix ceramic materials, Journal of Alloys and Compounds 473 (1–2) (2009) 190–194.
[37] C.P. Ostertag, Influence of fiber and grain bridging on crack profiles in SiC fiber-reinforced alumina-matrix composites, Materials Science and Engineering: A 260 (1–2) (1999) 124–131.
[38] D.X. Tang, H.B. Lim, K.J. Lee, C.H. Lee, W.S. Cho, Evaluation of mechanical reliability of zirconia-toughened alumina composites for dental implants, Ceramics International 38 (3) (2012) 2429–2436.
[39] K. Kalaitzidou, H. Fukushima, L.T. Drzal, Multifunctional polypropylene composites produced by incorporation of exfoliated graphite nanoplatelets, Carbon 45 (7) (2007) 1446–1452.
[40] S.W. Kim, W.S. Chung, K.S. Sohn, C.Y. Son, S. Lee, Improvement of flexure strength and fracture toughness in alumina matrix composites reinforced with carbon nanotubes, Materials Science and Engineering: A 517 (1–2) (2009) 293–299.
[41] J. Dusza, J. Morgiel, A. Duszova, L. Kvetkova, M. Nosko, P. Kun, C. Balazsi, Microstructure and fracture toughness of Si_3N_4+graphene platelet composites, Journal of the European Ceramic Society 32 (1–2) (2012) 3389–3397.
[42] P. Kun, O. Tapaszto, F. Weber, C. Balazsi, Determination of structural and mechanical properties of multilayer graphene added silicon nitride-based composites, Ceramics International 38 (1) (2012) 211–216.